CHEMISTRY
A EUROPEAN JOURNAL

DOI: 10.1002/chem.200700867

Metal-Catalysed Oxidation Processes in Thiosemicarbazones: New Complexes with the Ligand *N*-{2-([4-*N*-Ethylthiosemicarbazone]-methyl)phenyl}-*p*-toluenesulfonamide

Rosa Pedrido,[a] María J. Romero,[a] Manuel R. Bermejo,*[a] Ana M. González-Noya,[b] Iria García-Lema,[c] and Guillermo Zaragoza[d]

Abstract: The coordination behaviour of a new thiosemicarbazone Schiff-base building block, *N*-{2-([4-*N*-ethylthiosemicarbazone]methyl)phenyl}-*p*-toluenesulfonamide, H_2L^1 (**1**), incorporating a bulky tosyl group, towards Mn^{II}, Fe^{II}, Co^{II}, Ni^{II}, Cu^{II}, Zn^{II}, Cd^{II}, Ag^{I}, Sn^{II}, and Pb^{II} has been investigated by means of an electrochemical preparative procedure. Most metal complexes of L^1 have the general formula $[M(L^1)]_2{\cdot}nX$ (M = Mn, Fe, Co, Ni, Cu, Cd, Pb; $n = 0$–4, $X = H_2O$ or CH_3CN), as confirmed by the structure of $[Pb(L^1)]_2$ (**15**), in which the lone pair on lead is stereochemically active. This lead(II) complex shows an intense fluorescence emission with a quantum yield of 0.13. In the case of silver, the complex formed was found to possess a stoichiometry of $[Ag_2(L^1))]_2{\cdot}3\,H_2O$. During reactions with manganese and copper metals, interesting catalysed processes have been found to take place, with remarkable consequences regarding the ligand skeleton structure. In synthesising the manganese complex, we obtained an unexpected dithiolate thiosemicarbazone tosyl ligand, H_2L^2, as a side-product, which has been fully characterised, including by X-ray diffraction analysis. In the case of copper, the solid complex has the formula $[CuL^1]_2$, but the crystallised product shows the copper atoms coordinated to a new cyclised thiosemicarbazone ligand, H_2L^3, as in the structures of the complexes $[Cu(L^3)]_2{\cdot}CH_3CN$ (**8**) and $[Cu(L^3)(H_2O)]_2{\cdot}CH_3CN{\cdot}H_2O$ (**9**). The zinc complex $[Zn(L^1)]_4$ (**12**) displays a particular tetranuclear zeolite-type structure capable of hosting small molecules or ions, presumably through hydrogen bonding.

Keywords: cyclisation · dithiolate ligands · electrochemistry · fluorescence · multinuclear NMR · thiosemicarbazones

Introduction

Thiosemicarbazones are unique and versatile ligands, not only because they possess a great variety of donor sets and high versatility in terms of their coordination,[1] but also due to the fact that they show varied biological, structural, and optical properties.[2,3] It is now firmly established that their transition metal complexes are potent pharmacological agents,[4] generally showing higher activity than the parent thiosemicarbazones.[5] This feature is currently being studied in order to establish their role at the DNA level. It has been suggested that thiosemicarbazone compounds block DNA biosynthesis,[6] while other studies indicate that they act as DNA intercalating agents.[7]

Electrochemical procedures have been widely used for the synthesis of metal complexes, especially in cases where the organic ligands contain donor groups with weak acidity.[8] The conditions employed in this experimental methodology have proved suitable for deprotonating amide func-

[a] Dr. R. Pedrido, M. J. Romero, Prof. Dr. M. R. Bermejo
Departamento de Química Inorgánica, Facultade de Química, Universidade de Santiago de Compostela
15782 Santiago de Compostela (Spain)
Fax: (+34) 981-597-525
E-mail: qimb45@usc.es

[b] Dr. A. M. González-Noya
Departamento de Química Inorgánica
Facultade de Ciencias, Universidade de Santiago de Compostela
27002 Lugo (Spain)

[c] I. García-Lema
Departamento de Química Física
Facultade de Química
Universidade de Santiago de Compostela
15782 Santiago de Compostela (Spain)

[d] G. Zaragoza
Unidade de Difracción de Raios X, Edificio CACTUS
Universidade de Santiago de Compostela, Campus Sur
15782 Santiago de Compostela (Spain)

Supporting information for this article is available on the WWW under http://www.chemeurj.org/ or from the author.

tions and thus it provides an easy and inexpensive synthetic procedure whereby complexes may be formed in the absence of external coordinating species. It is well known that the use of acid metal salts facilitates complex formation by coordination of the metal to the protonated organic substrate, the coordination of undesired anions being quite common. We have demonstrated that the appending of a tosyl group to an amide-type Schiff-base ligand increases the acidity of the amide hydrogen, thereby making the ligand more anionic in nature. Furthermore, a tosyl group increases the solubility of the ligand and its metal complexes.[9] In addition, the presence of additional donor atoms in the amide ligand may allow the formation of stable five- and six-membered chelate rings with a metal ion, and this may make the metal complexation easier.

In previous work, we have employed Schiff-base ligands derived from thiosemicarbazones[10,11] or containing tosyl groups[9] as useful building blocks for the construction of polynuclear helicates. As a result of our interest in the design of organic systems suitable for the assembly of supramolecular compounds, we decided to incorporate these two molecular motifs in the same ligand to afford combined thiosemicarbazone and tosylamide skeletons. As a consequence, we have synthesised a new thiosemicarbazone Schiff-base ligand (Scheme 1) by incorporating a bulky tosyl

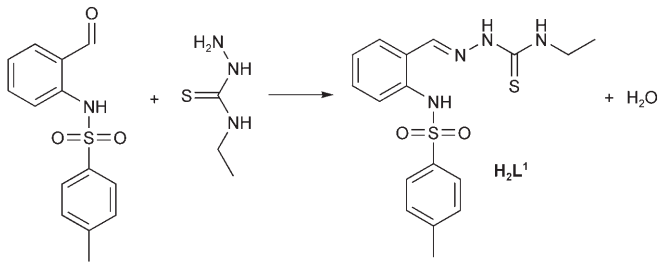

Scheme 1. Synthesis of the ligand H_2L^1.

group. The interactions of this ligand with transition and post-transition metals have been investigated by means of an electrochemical preparative method. The results obtained are reported herein.

Results and Discussion

Synthesis of the ligands: The Schiff base H_2L^1 was prepared according to a four-step synthetic route in an overall yield of 50%. The first three steps relate to the synthesis of 2-tosylaminobenzaldehyde.[12]

Treatment of 2-tosylaminobenzaldehyde with 4-*N*-ethyl-3-thiosemicarbazide in a 1:1 molar ratio under reflux conditions in ethanol yielded the $[N_2S]$ tridentate Schiff-base ligand H_2L^1 (Scheme 1). The soft white powdery solid formed was satisfactorily characterised, as detailed in the Experimental Section.

The new dithiolate Schiff base H_2L^2 (Scheme 2) was very easily obtained by concentration of the mother liquor from an electrochemical synthesis involving manganese, followed by slow recrystallisation of the residue obtained from a dichloromethane/diethyl ether mixture. The soft yellow crystalline product was fully characterised, again as detailed in the Experimental Section.

Synthesis of the complexes: New neutral metallic complexes were obtained by electrochemical oxidation of appropriate metal anodes in an acetonitrile solution containing the ligand H_2L^1 in the presence of a small quantity of tetraethylammonium perchlorate as supporting electrolyte. Electrochemical efficiency values for the cells with the M^{II} complexes were around $0.5\,mol\,F^{-1}$, while for the Ag^I complex the value was $0.9\,mol\,F^{-1}$, according to the following mechanism:

$$\text{cathode}: [H_2L^1] + 2e^- \rightarrow H_2(g) + [L^1]^{2-}$$

$$\text{anode}: [L^1]^{2-} + M \rightarrow [M(L^1)] + 2e^-$$

$$\text{anode}: [L^1]^{2-} + 2Ag \rightarrow [Ag_2(L^1)] + 2e^-$$

Several attempts to obtain the tin complex, under various electrochemical conditions, yielded only complicated uncharacterisable mixtures.

Analytical and spectroscopic data: The aforementioned electrochemical procedure allowed us to easily obtain neutral complexes of the type $[M(L^1)]_2{\cdot}nX$ (M = Mn, Fe, Co, Ni, Cu, Cd, Pb; n = 0–4, X = H_2O or CH_3CN), $[Ag_2(L^1)]_2{\cdot}3H_2O$, and $[Zn(L^1)]_4{\cdot}2H_2O$, in high purities and very good yields.

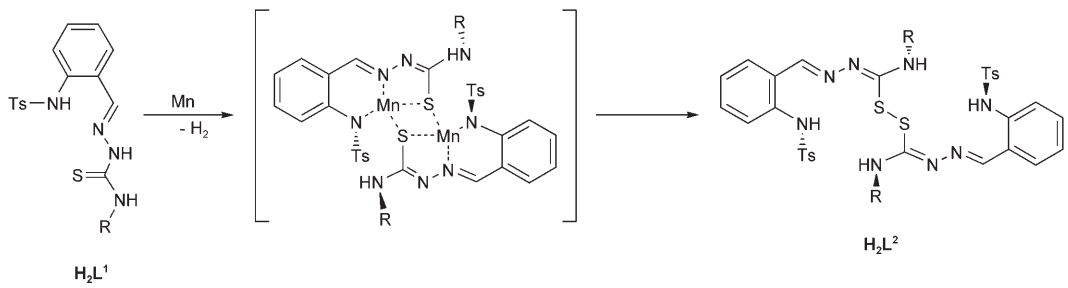

Scheme 2. Proposed mechanism for the formation of the disulfide ligand H_2L^2.

All of the obtained complexes are air-stable as well as thermally stable, melting above 300 °C without decomposition. The molar conductivity values of these compounds are consistent with non-electrolyte character. The magnetic moments for the Mn, Fe, Co, Ni, and Cu complexes are quite similar to those expected for magnetically diluted M^{II} ions, which confirms that the ligand acts in a fully deprotonated form, $[L^1]^{2-}$.

Mass spectrometry and IR spectroscopy: The FAB mass spectra of the complexes show peaks due to the fragments $[M(L^1)]_n$, indicative of the coordination of the ligand H_2L^1 to the different metals and suggesting a polynuclear nature for all of these complexes. Fragments containing solvent molecules were not always observed, reflecting the solvating rather than coordinating behaviour of the solvent molecules. In order to assess the identity and the nuclearity of the complex species formed in solution, ESI-MS experiments were performed for all of the complexes. The spectra of the manganese, iron, cobalt, nickel, copper, cadmium, and lead complexes feature peaks corresponding to $[M_2(L^1)_2+H]^+$ fragments, suggesting that the dinuclear complexes are the main species in solution. On the other hand, the spectrum of the silver compound shows peaks corresponding to $[Ag_2(L^1)+H]^+{}_2$, which confirms the stoichiometry suggested by the analytical data. In the case of zinc, peaks corresponding to $[Zn_4(L^1)_4+H]^+$ were detected, implying that the tetranuclear nature of this complex seen in the solid state (X-ray studies; see below) might also be maintained in solution.

The IR spectra of the complexes show that the shift of charge caused by the coordination of the imine and thiol groups to the metal centre leads to a general displacement of the ν(C=N+C−N) and ν(C−S) bands in comparison with those of the free ligand. The bands assigned to the asymmetric and symmetric vibrational modes of SO_2 groups[13,14] are also slightly shifted. These data are compatible with the participation of the imine and amide nitrogen atoms as well as the sulfur atoms in coordination to the metal centres.

No bands at around 3151 cm^{-1} are seen for these complexes, indicating complete deprotonation of the amide and thiosemicarbazide NH groups, thereby confirming the dianionic character of the ligand H_2L^1.

NMR spectroscopy: The ^1H NMR spectra of the free ligand H_2L^1 and its silver, zinc, cadmium, and lead complexes were recorded in [D_6]DMSO at room temperature. The spectra of these complexes do not show significant changes with temperature. All of the spectra, except for that of the silver complex, show a single set of signals, which could be completely assigned. This fact implies that there are single species in solution. Comparison of the ^1H NMR spectrum of the free ligand with those of the complexes (Figure S1, Supporting Information) shows some interesting aspects. 1) The imine proton signal (H4) is shifted upfield for the silver, zinc, cadmium, and lead complexes. This signal is flanked by satellites arising from spin-spin coupling to $^{111/113}Cd$ in the spectrum of the cadmium complex, indicating that this complex is kinetically inert on the NMR timescale. 2) The spectra of the silver, zinc, cadmium, and lead complexes show an absence of the NH proton signals seen for the free ligand (H1 at $\delta = 11.5$ ppm and H2 at $\delta = 9.9$ ppm), confirming the twofold deprotonation of the ligand in these complexes. 3) The signal of the thioamide NH proton (H3 at $\delta =$ 8.5 ppm in the free ligand) is strongly shifted upfield in all of these complexes, as we have found in other thiosemicarbazone complexes.[11] 4) The signals of the aromatic protons of the tosyl and benzylidene rings are also shifted on complexation. 5) The presence of some low intensity signals in the spectrum of the silver complex, in the region $\delta = 8.0$–11.0 ppm, may be indicative of the existence of an equilibrium between different species in solution. This equilibrium might be the consequence of a gradual demetallation process as the intensity of the secondary signals increases with time and it may be indicative of low stability of this complex in DMSO solution.

The ^1H NMR spectrum of the disulfide ligand H_2L^2 was also recorded in [D_6]DMSO at room temperature and compared with that of the parent ligand H_2L^1, as illustrated in Figure 1. This spectrum shows that the formation of the disulfide bond generates a completely symmetrical ligand, the signal of the NH proton H2 disappearing and that of the thioamide NH proton H3 being notably shifted. The other signals are slightly shifted upfield (H1 and H5) or downfield (H4, H6, H8, and H10). The signals of the aliphatic protons do not display any significant changes.

In order to explore the solution behaviour of the cadmium and lead complexes, we recorded their ^{113}Cd and ^{207}Pb NMR spectra, respectively.

The ^{113}Cd NMR spectrum of $[Cd(L^1)]_2 \cdot CH_3CN$ (**13**) in [D_6]DMSO solution shows only one signal at $\delta = 258$ ppm (Figure S2, Supporting Information). It is well known that the shielding of the $^{113}Cd^{II}$ nucleus increases in the order O > N > S when the donor atoms are changed and/or when the coordination number is increased.[15] This effect is illustrated by comparing the ^{113}Cd chemical shifts exhibited by the complex [Cd(H_2DAPTsz-Me)], derived from a pentadentate thiosemicarbazone [N_3S_2] ligand ($\delta = 305$ ppm),[11a] and complex **13** presented here, coordinated through the [N_2S] donor system of a ligand unit and probably by one N of a second ligand which results in a tetracoordinated [N_3S] environment for the Cd metal ion ($\delta = 258$ ppm).

The dependence of the ^{207}Pb NMR[16] parameters on the Pb^{II} coordination environment has not been fully established.[17,18] The lead(II) complex **14**, with a core of [N_3S], shows a single signal at $\delta = -237$ ppm (Figure S2, Supporting Information). This value seems to be in line with expectation for this complex with a lead(II) [N_3SO] pentacoordinated environment. Since this complex is tetracoordinated [N_3S] in the solid state, the value obtained in DMSO solution may be indicative of the coordination of one DMSO molecule to the structure seen in the solid state, with the lone pair on lead being stereochemically active. Moreover, this value is also consistent with a more shielded value when S is substituted by O, keeping the coordination number con-

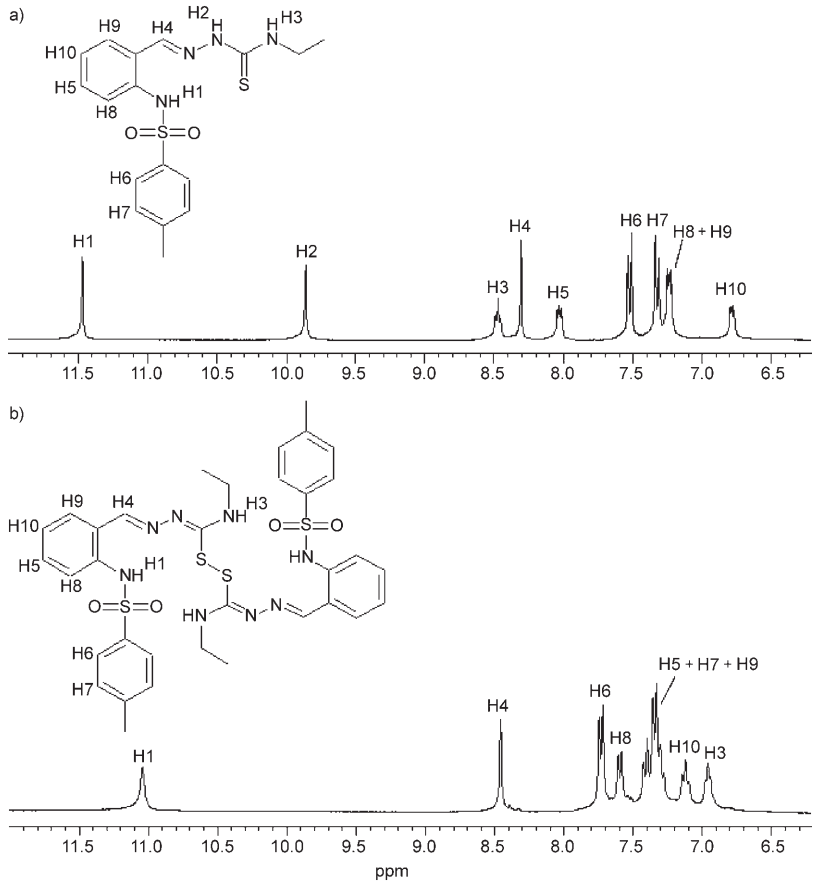

Figure 1. ^{1}H NMR spectra of the ligand H_2L^1 (a) and the new disulfide ligand H_2L^2 (b) in [D_6]DMSO.

stant, if we compare it with an [N_3S_2] pentacoordinated lead(II) complex derived from a pentadentate thiosemicarbazone.[11a]

UV/Vis absorption and fluorescence emission studies: The electronic absorption spectra of the ligands and metal complexes show intense bands in the near-UV region ($\varepsilon = 10^4$–$10^5\,mol^{-1}\,dm^3\,cm^{-1}$), indicative of highly conjugated π-systems. The characteristic two bands due to the π→π* absorption of the tosyl groups, appearing at around 225 and 250 nm in the free ligands, are red-shifted and their intensities are increased in all of the complexes. Additionally, the spectrum of the ligand H_2L^1 (**1**) shows a single broad charge-transfer (CT) band at 320 nm due to n→π* absorption associated with p-π conjugation of the nitrogen lone-pair electrons with the aromatic systems. In the case of its metal complexes, additional bands appear in the range 300–390 nm attributable to ligand-to-metal charge transfer (LMCT). On the other hand, four broad CT bands appear in the spectrum of the disulfide ligand H_2L^2 (**3**) in the region 300–350 nm.

The incorporation of the fluorophore 2-tosylaminobenzaldehyde ($\lambda_{em} = 498$ nm) into the ligands **1** and **3** allowed us to study their ability to serve as fluorescent chemosensors for transition and heavy metal ions. The fluorescence emission spectra of both ligands and all of the metal complexes were recorded from 4×10^{-7} M solutions in acetonitrile.

H_2L^1 (**1**) and H_2L^2 (**3**) do not show fluorescence emission, probably due to quenching by an intramolecular photoinduced electron transfer (PET) process involving the unpaired electrons of the nitrogen atoms.[19]

Upon excitation at the corresponding absorption maxima, the zinc, cadmium, and lead complexes show intense fluorescence emissions with quantum yields of 0.05, 0.03, and 0.13, respectively, while no fluorescence enhancement was observed for the transition metal complexes (Figure S3, Supporting Information). The fluorescence emission in these complexes can be explained in terms of a conformational change of the ligand H_2L^1 as well as inhibition of the PET process by coordination of the nitrogen atoms to the metal ions.[19,20] Therefore, the different emission intensities depend on the delocalization of charge through the vacant orbitals of each metal centre.[21]

The emission spectra of the complexes $[Zn(L^1)]_4\cdot 2H_2O$ (**11**), $[Cd(L^1)]_2\cdot CH_3CN$ (**13**), and $[Pb(L^1)]_2\cdot 3H_2O$ (**14**) each show a single broad band, with the maxima at 490 nm (Zn and Pb) and 486 nm (Cd). The spectra are independent of the excitation monitoring wavelength, suggesting the presence of a single emissive species in the excited state. The consistency of these values confirms that the twofold deprotonated ligand adopts the same conformational arrangement in coordinating to these metal centres, in agreement with the results obtained by X-ray diffraction analysis.

X-ray diffraction studies

Crystal structures of the ligands H_2L^1 (1) and H_2L^2 (3): The crystal structure of the ligand H_2L^1 (**1**) reveals that the thiosemicarbazone exists as discrete molecules (Figure 2). The thiosemicarbazone arm adopts an *E* conformation about the imine bond in order to minimise unfavourable electronic interactions with the bulky tosyl group. As expected, the disposition of this molecule in the solid state is controlled by the presence of two intramolecular hydrogen bonds between the amine and imine [N1−H1···N2, 2.678(2) Å] and the imine and thioamide nitrogen atoms [N4-H4···N2, 2.641(7) Å], respectively. Significant intermolecular interac-

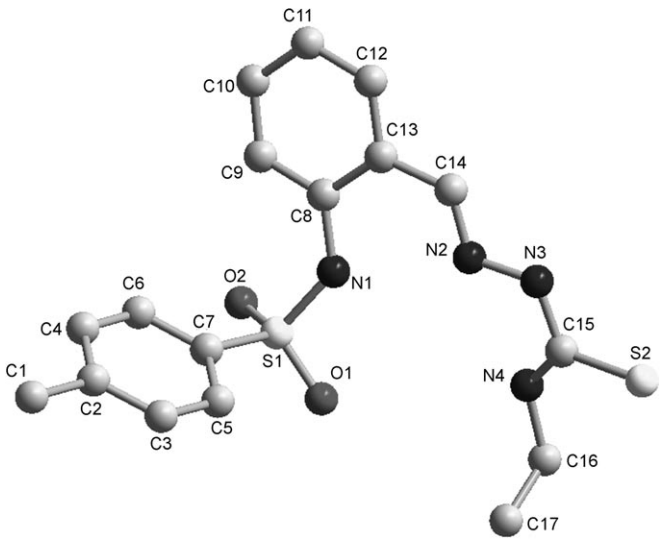

Figure 2. Crystal structure of the ligand H_2L^1 (**1**).

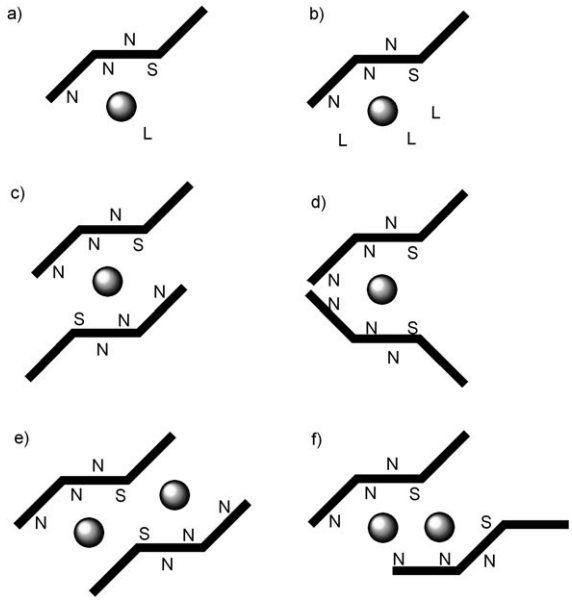

Scheme 3. Possible coordination modes for the building block H_2L^1.

tions through hydrogen bonds can also be observed between the thioamide sulfur atom of one ligand thread and the hydrazide nitrogen atom of a neighbouring molecule [N3–H3···S2, 3.3879(18) Å; $1-x$, $-y$, $-z$], giving rise to the association of two H_2L^1 units (Figure S4, Supporting Information).

The conformation shown for this ligand must undergo a significant change to allow the thioamide sulfur atom to coordinate to the same metal centre, so that the ligand can act as a potentially tridentate and dianionic building block. As the coordination of the [N_2S] donor set of the twofold deprotonated ligand will not be enough to satisfy the coordinative requirements of the majority of transition or post-transition metal atoms, different coordinative situations must arise (Scheme 3):

1) One ligand thread [N_2S] may be exclusively coordinated to one metal ion, so that the metal coordination number is completed by additional ligands L (e.g., solvent molecules) that occupy the remaining coordination sites (a, b).
2) Two ligand units, partially or fully deprotonated depending on the oxidation state of the metal, may be bound to the same metal ion in a *syn* or *anti* arrangement (c, d).
3) Two ligands may coordinate to two or more metal ions with the establishment of bridging bonds via the sulfur or the hydrazide nitrogen atoms (e, f).

A view of the crystal structure of the new disulfide ligand H_2L^2 (**3**) is shown in Figure 3. This new compound can be described as two H_2L^1 units linked by an S–S bond involving the thiosemicarbazone sulfur atoms. The crystal structure reveals that H_2L^2 exists as discrete molecules showing an *anti*-conformation about the central disulfide bond, and retaining the *E* conformation about the imine bonds (as in the ligand H_2L^1) in order to minimise unfavourable electronic interactions with the bulky tosyl group.

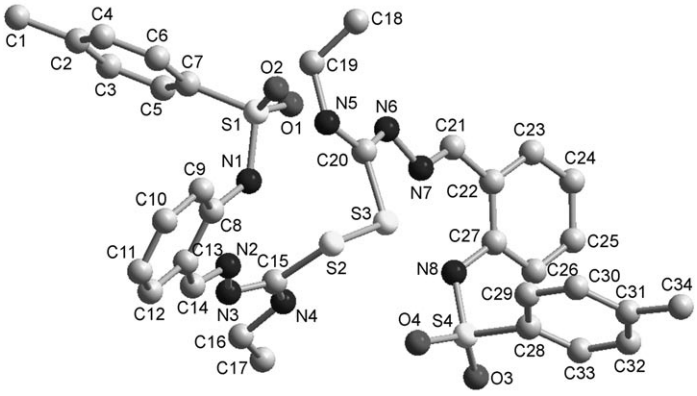

Figure 3. Crystal structure of the disulfide ligand H_2L^2 (**3**).

As expected, the conformational arrangement is controlled by the presence of intramolecular hydrogen bonds (Figure S5, Supporting Information), involving the amide nitrogen, thioamide nitrogen, tosyl oxygen, and disulfide sulfur atoms [N4–H4A···S3 3.049(4), N1–H1···N2 2.66(5), N5–H5A···S2 3.073(3), N5–H5A···O1 2.926(4), N8–H8A···N7 2.926(4) Å].

The S–S bond length in H_2L^2 [S2–S3 2.039(1) Å] and the C15-S2-S3-C20 torsion angle of 93.4(1)° are essentially similar to those observed in other organic disulfide ligands.[22] The torsion angles N4-C15-S2-S3 [16.9(4)°] and S2-S3-C20-N6 [172.9(2)°] are, within the range found in most disulfides with an equatorial conformation, closer to 0 or 180° according to the Shefter classification[23] (ca. 0 or 180° for equatorial and 90° for axial conformations). This means that both

sulfur atoms lie approximately in the plane of the N-N-C-N thiosemicarbazone skeleton to which they are bound (0.0267 and 0.0319 Å). In addition, according to the criteria of Higashi et al.,[24] the equatorial conformation is also confirmed by the S2–S3 distance, which is shorter than the typical axial range (2.060–2.108 Å), and the C-S-S angles [C15-S2-S3 103.3(8) and C20-S3-S2 104.5(8)°], which are larger than those in other organic disulfides showing an axial conformation (100–103°).

Formation of disulfide ligands by oxidation of thiosemicarbazones: The oxidation of thioamides (RNHCS-R) and organo-thiols (RSH) by metal ions (mainly by copper(II) and iron(III)) are well-known processes,[25] both of which are of technological and biochemical interest.[26] In these reactions, the S–S bond may be formed after the addition of some external oxidant or following reduction of the metal ions. For example, the reactions of copper(II) with thiolates usually lead to a reduction of the cation with the consequent formation of RSSR and copper(I) species, followed by re-oxidation of the latter to copper(II) in the presence of O_2.[27] On the other hand, in some cases, reactions involving disulfides can be reversible, involving breakage of the disulfide bond under reductive conditions to yield thiolate complexes.[28] Interconversion between disulfide and the corresponding thiolate is a very important redox process at the biological level,[26,27] but the factors controlling this process are still not well understood. Processes of this kind have attracted a great deal of interest, as evidenced by the extensive literature concerning the oxidation of thioamides or thioureas to disulfide compounds.[29]

The disulfide ligand H_2L^2 presented here was formed by an oxidation process of the initial thiosemicarbazone ligand H_2L^1 during experiments on the electrochemical synthesis of the manganese complex. The proposed mechanism could start after the establishment of a thione–thiol equilibrium in solution, with the coordination of manganese atoms to two different doubly-deprotonated ligand units acting as $[N_2S]$ donor sets and coordination of the thiolate sulfur atom as a μ_2-bridge between the two metals.[30] This step is followed by a reductive elimination process resulting in the coupling of two thiolate units, thereby creating the disulfide link. This mechanism is summarised in Scheme 2.

Such an oxidation process leading to a disulfide has been observed previously using an electrochemical methodology for the synthesis of metal complexes, but with heterocyclic thione-type ligands.[31] With the latter, it was found that the oxidation to disulfide only occurred when the thione compound was the only ligand present in solution, since the presence of co-ligands inhibited the S–S coupling.

In our work, the oxidation of the thiosemicarbazone to disulfide under physiological conditions could lead to a reinterpretation of the biological properties of some thiosemicarbazone systems, primarily those aspects related to their possible therapeutic uses.

Finally, this process is totally reproducible and opens up an easy way of acquiring a library of new disulfide ligands. Further work to develop and extend this methodology is already in progress.

Crystal structures of $[Cu(L^3)]_2{\cdot}CH_3CN$ (8) and $[Cu(L^3)(H_2O)]_2{\cdot}CH_3CN{\cdot}H_2O$ (9): The molecular structures of these complexes are shown in Figure 4 and Figure S6 (Supporting Information), together with the atom numbering scheme adopted. The main bond lengths and angles are given in Table 1.

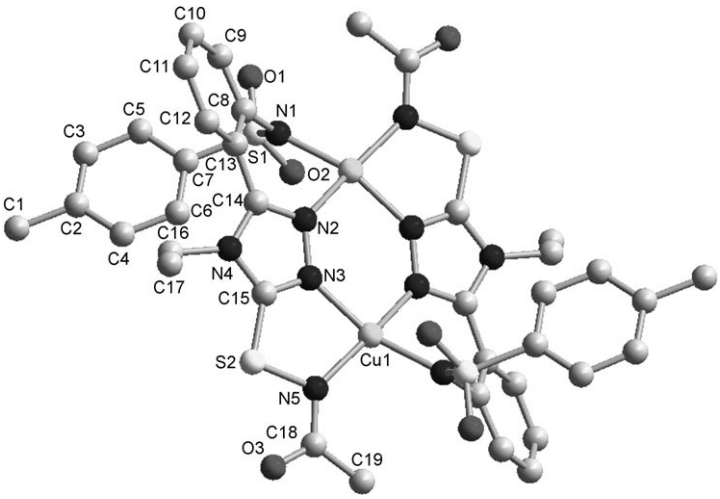

Figure 4. Molecular structure of the complex $[Cu(L^3)]_2{\cdot}CH_3CN$ (**8**).

The new complexes can be described as dimers in which two new cyclised ligand molecules H_2L^3 (see Scheme 4), doubly-deprotonated in a head-to-tail arrangement, are coordinated to two copper(II) atoms. Both complexes are solvated by solvent molecules, by acetonitrile in the case of complex **8** and by one acetonitrile and one water molecule in the case of complex **9**.

Oxidative cyclisation of the original ligand H_2L^1 by Cu^{2+} ions followed by the addition of an acetamide fragment accompanied by a reductive elimination process led to the formation of the new tetradentate ligand H_2L^3. The new ligand features a central five-membered 1,2,4-triazole ring C15-N4-C14-N2-N3, formed by nucleophilic attack of the thioamide nitrogen (N4) on the imine carbon (C14) (Scheme 4), followed by the addition of an acetamide fragment to a Cu^{2+} ion and the sulfur atom. The formation of the latter bond can be explained by the existence of thiol–thione tautomerism of the thione sulfur atom, taking into account the fact that only the thiol form can exist in solution. The attachment of the acetamide fragment leads to changes in the coordination behaviour of the new cyclised ligand H_2L^3, as the sulfur atom cannot act as a donor site for the coordination of the metal atoms as is the case in most 1,2,4-triazole-3-thione complexes.[32] Instead, a new terminal amide NH is incorporated into the skeleton. All these processes ultimately result in the formation of a new $[N_4]$ ligand coordinated to two Cu^{II} metal ions in a doubly-deprotonated mode.

Table 1. Main bond lengths [Å] and angles [°] for **8**, **9**, and **15**.

$[Cu(L^3)]_2{\cdot}CH_3CN$ (**8**)		$[Cu(L^3)(H_2O)]_2{\cdot}CH_3CN{\cdot}H_2O$ (**9**)		$[Pb(L^1)]_2$ (**15**)	
Cu1–N1	1.946(4)	Cu1–N1	1.991(2)	Pb1–N3	2.618(3)
Cu1–N2	1.983(4)	Cu1–N2	1.993(2)	Pb1–N1	2.459(3)
Cu1–N3	1.964(4)	Cu1–N3	2.003(2)	Pb1–N2	2.426(3)
Cu1–N5	1.976(4)	Cu1–N5	1.994(2)	Pb1–S2	2.724(1)
S1–N1	1.588(3)	Cu1–O(4)	2.254(2)	S1–N1	1.576(3)
C7–S1	1.757(4)	S1–C7	1.770(2)	N1–C8	1.408(4)
C14–N4	1.360(4)	N1–S1	1.590(2)	C14–N2	1.283(4)
C15–N4	1.347(4)	C14–N4	1.370(2)	N2–N3	1.399(3)
C15–S2	1.705(4)	C15–N4	1.358(2)	C15–S2	1.734(3)
N2–N3	1.381(4)	N3–N2	1.382(2)	N3–C15	1.323(4)
S2–N5	1.715(3)	S2–C15	1.732(2)	C15–N4	1.338(4)
C18–N5	1.336(4)	N5–S2	1.727(2)		
N1-Cu1-N2	84.9(1)	N5–C18	1.342(2)	N2-Pb1-N1	70.85(9)
N1-Cu1-N5	84.4(1)	N1-Cu1-N2	85.53(6)	N2-Pb1-S2	70.56(6)
N3-N2-Cu1	128.0(2)	N1-Cu1-N5	98.11(6)	N1-Pb1-N3	117.29(8)
N3-Cu1-N5	84.4(1)	N5-Cu1-N3	84.09(6)	N1-Pb1-S2	114.64(7)
N3-N2-Cu1	135.3(2)	N5-Cu1-O4	89.57(7)	N2-Pb1-N3	71.22(8)
C8-N1-S1	120.5(2)	N3-Cu1-O4	104.86(3)	C8-N1-S1	123.5(2)
N2-C14-C13	124.9(3)	C8-N1-S1	117.3(1)	C14-N2-N3	112.9(3)
C15-N3-N2	106.7(2)	N2-C14-C13	125.0(2)	N3-C15-S2	126.8(2)
N4-C15-S2	125.03(2)	C15-N3-N2	106.9(1)	N4-C15-S2	119.2(3)
		N4-C15-S2	125.3(1)		

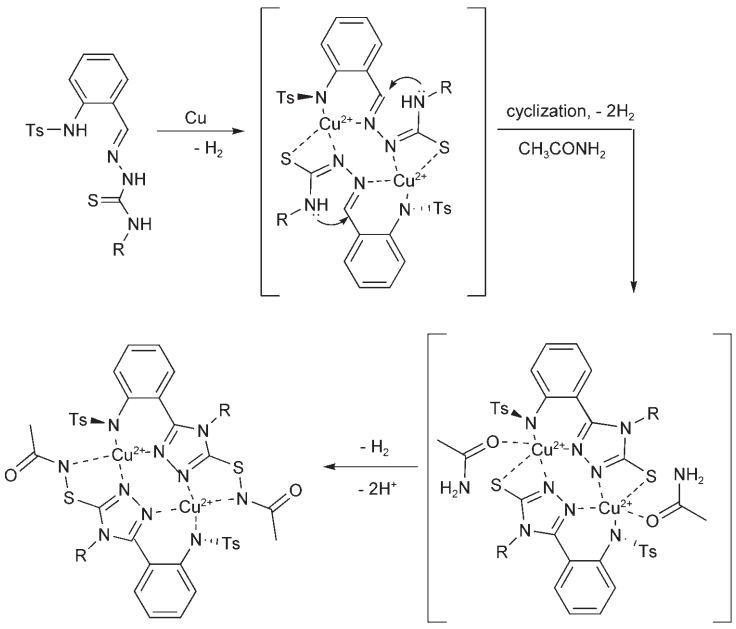

Scheme 4. Proposed mechanism for the formation of **8** and **9** by copper-catalysed oxidative cyclization of the ligand H_2L^1 followed by addition of an acetamide group.

The existence of an acetamide fragment in the reaction medium may possibly be explained in terms of copper-catalysed hydrolysis of acetonitrile.[33] Nitriles are compounds that are very stable under normal conditions and they are usually used as safe organic solvents. However, in recent years, the hydrolysis of nitriles to amides is a reaction that has attracted much attention. It has been found that some transition metal ions can catalyse their hydrolysis very efficiently, including complexes of bivalent metals Cu^{II}, Ni^{II}, Zn^{II}, Pt^{II}, Rh^{II}, and Pd^{II}, as well as trivalent metals Co^{III}, Rh^{III}, Ru^{III}, and Ir^{III}.[34]

The attachment of an acetamide fragment to the formed 1,2,4-triazole-3-thione ring has not been reported previously and it seems to take place under the catalytic action of the copper ions in the work presented here. Coordination of the metal followed by reductive elimination gives rise to the formation of a new covalent S–N bond.[35]

In these two new complexes, the new cyclised ligand $[H_2L^3]$ is tetradentate and dianionic. Two different ligand molecules coordinate both copper atoms. Each ligand thread uses the amide nitrogen and one of the triazole nitrogen atoms to coordinate one of the copper atoms, and uses the remaining triazole and acetamide nitrogen atoms to coordinate the second metal. This coordinative behaviour results in complex **8** containing both copper atoms in a tetracoordinated environment with a distorted square-planar geometry. The distortion from this geometry is clearly shown by the angles subtended by copper and the donor atoms of the ligands, with values between 84.39° and 101.25°, quite different from the ideal value (90°) for this geometry.

In the case of complex **9**, the additional coordination of a water molecule provides a new pentacoordinated environment for each copper atom that can be described in the solid state as intermediate between square-planar pyramidal (SP) and trigonal-bipyramidal (TBP), as shown by a value of 0.49 for the τ parameter.[36]

Cyclisation of thiosemicarbazones: It is well known that semi- and thiosemicarbazones are polyfunctionalised compounds that easily cyclise under the action of bases,[37] acids,[38] oxidants,[39] or other cyclisation reagents,[40] and they are useful and versatile precursors for the preparation of five- or six-membered heterocyclic compounds. In fact, the oxidative cyclisation of thiosemicarbazones has been employed as an alternative to conventional organic synthesis and an inexpensive pathway for preparing ring-type molecules in one step. This approach makes a large variety of heterocycles accessible and offers very different conditions under which the reactions can be performed. Recently, it has been found that sometimes this ring-closure process may be induced by high-valence metal ions (Fe^{3+}, Cu^{2+}). The exact mechanism is still not well known, but it has been suggested that the influence of the metal ions on this process is probably due to both inductive and stereochemical effects.[41] Nevertheless, some difficulties arise in mechanistic

studies due to the Lewis acid nature of the metal cations, because of the possible formation of different substrate–cation complexes, and the inner-sphere nature of the electron-abstraction process. Under these circumstances, it is difficult to determine the exact steps of the reaction pathway experimentally as well as to identify the reaction intermediates, but more work needs to be done in order to build-up a thorough knowledge of reactions of this kind.

In the case of thiosemicarbazone ligands, the oxidative cyclisation mainly yields 1,2,4-triazole (A) or 1,3,4-thiadiazole (B) rings (Scheme 5), depending on the mechanism.[32,42] Based on a careful analysis of the available data, we surmise that the formation of the triazole ring could be induced by an attack of the oxidising agent on the tail-like thioamide moiety, followed by a single-electron transfer and then a rate-limiting ring-closure step. Alternatively, the thiadiazole heterocycle is formed as a result of an attack of the metal cation on the imine nitrogen atom, followed by a ring-closure step and finally an electron abstraction–dehydrogenation step.

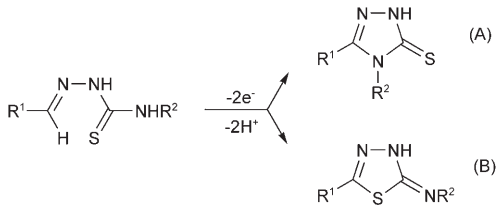

Scheme 5. Heterocyclic products of the cyclisation of thiosemicarbazones: A) 1,2,4-triazole-3-thione and B) 1,3,4-thiadiazole.

Other reported oxidation processes show the appearance of sulfate groups, which arise from oxidation of the thione sulfur atom[43] or desulfurisation of the thiosemicarbazone-copper(II) system by transformation of the thioamide group into a nitrile.[44]

All of these processes explain the versatility of thiosemicarbazone skeletons in supplying new organic and inorganic systems.

Molecular structure of $[Pb(L^1)]_2$ (15): The molecular structure of $[Pb(L^1)]_2$ (**15**) is shown in Figure 5, together with the atom numbering scheme adopted. The main bond lengths and angles are given in Table 1.

The crystalline structure of $[Pb(L^1)]_2$ (**15**) consists of a Pb^{II} dimer, in which two doubly-deprotonated ligand threads $[L^1]^{2-}$ coordinate two lead metal atoms in a box-type disposition.

Each lead atom is in a distorted $[N_3S]$ tetrahedral environment produced by the thioamide sulfur, amide nitrogen, and imine nitrogen atoms of the closest ligand unit. The coordination sphere of the lead atom is completed by the hydrazide nitrogen of a second ligand unit. This coordinative behaviour gives rise to two five-membered [Pb1-N2-N3-C15-S2], two six-membered [Pb1-N1-C8-C13-C14-N2], and a central third six-membered chelate ring [Pb1-N3-N2-Pb1-N3-N2], which confers stability to the system. The coordination number of four in lead complexes is quite unusual and only a few cases have been reported previously.[1] In particular, in the case of lead complexes with thiosemicarbazone ligands, we have found two complexes showing square or trigonal-pyramidal geometries for the lead atom, with the lone pair on lead being stereochemically active. This results in the non-spherical charge distribution around the Pb^{II} cation and it gives rise to a clear gap in the disposition of the ligand about the metal ion.[45] Recently, using a pentadentate thiosemicarbazone ligand with an $[N_3S_2]$ kernel, we reported the first example of a pentacoordinated lead complex clearly showing the "lone-pair effect".[11a]

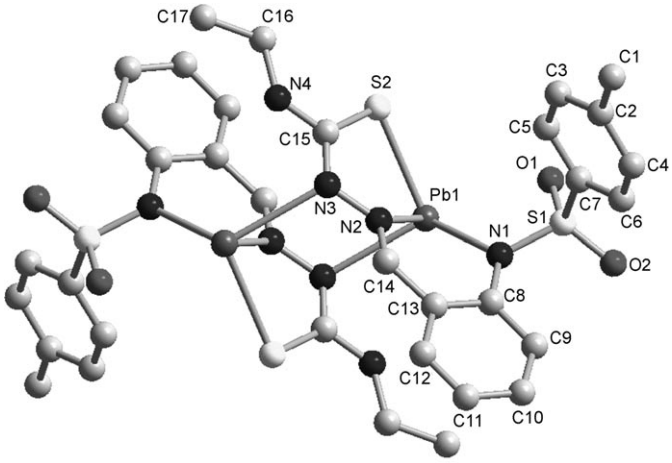

Figure 5. Crystal structure of the complex $[Pb(L^1)]_2$ (**15**).

Hancock et al. proposed that lead(II) complexes with a coordination number of less that eight should have Pb-N distances in the range 2.37–2.56 Å.[46] Two of the three Pb-N distances in our complex **15** are consistent with Hancock's proposal of the existence of a stereochemically active lone pair [Pb1–N1 2.459(3), Pb1–N2 2.426(2) Å]. The third one is out of the range [Pb1–N3 2.618(3) Å], because it relates to a faraway ligand unit.

The absence of additional ligands in the free apical position could be also controlled by the possible existence of a secondary intramolecular interaction between the lead atom and one of the tosyl oxygens due to the short bond length [Pb1–O1, 2.9088(24) Å]. With this fact in mind and considering the existence of the stereochemically active lone pair, the environment about the lead atom can alternatively be described as distorted octahedral, with four positions being occupied by the $[N_3S]$ donor set provided by the two doubly-deprotonated ligands $[L^1]^{2-}$, and the O1 tosyl oxygen atom and the lone pair on lead completing the six-coordinated environment.

The distortion of the coordination polyhedron is further reinforced by the deviation from planarity of the Pb atom and the $[N_3S]$ donor set of the nearest ligand. The maximum deviation from the $[N_3S]$ least-squares calculated plane is 0.0610 Å, with the lead 1.3745 Å above this plane. This distortion of the lead atom in **15** is greater than that in other

complexes showing the "lone-pair effect" that we have prepared previously.[11a,47]

NMR studies are in agreement with these results and suggest that the lone-pair effect around the lead(II) also persists in solution.

Molecular structure of $[Zn(L^1)]_4$ (12): Recrystallisation of the solid compound $[Zn(L^1)]_4 \cdot 2H_2O$ (**11**) from different solvent mixtures gave single yellow plates of relatively poor quality, which could nevertheless be characterised by single-crystal X-ray analysis. The NMR spectra of the crude and recrystallised materials were similar. The quality of the data did not allow refinement to a satisfactory level, although we trust the gross structural features. All attempts to subsequently grow better quality crystals have been unsuccessful.

The structure of this zinc complex is presented in Figure 6. The complex consists of a supramolecular tetranuclear array of zinc atoms on the vertices of a square parallelogram (Zn-Zn angles are close to 90°). This parallelogram is nearly planar and the distances between contiguous zinc atoms are of the order of 4.7 Å. This coordination mode creates a distorted square cavity with smaller dimensions (of the order of 4 Å) than the distance between metal centres due to the fact that the thiosemicarbazone chains are slightly oriented towards the interior hole. This particular self-assembly generates a supramolecular 2D network (Figure 7) in the crystal cell that resembles the structure of zeolites[48] and, indeed, it could be suitable for hosting small molecules or ions through hydrogen bonds.

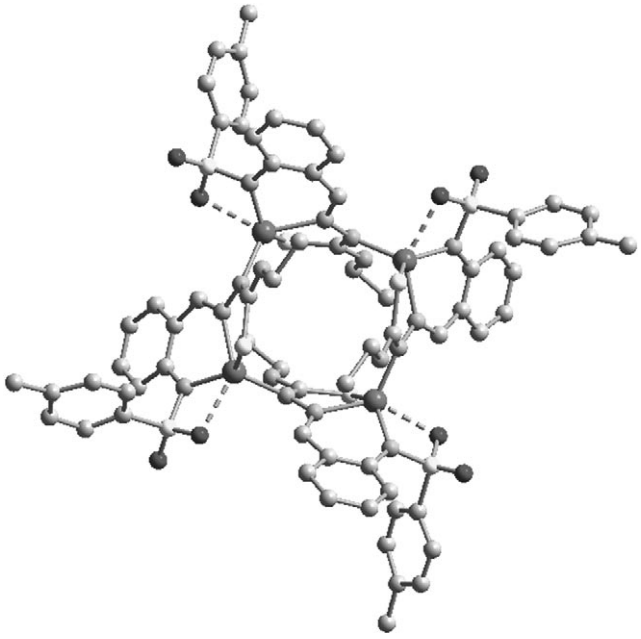

Figure 6. Molecular structure of the tetranuclear complex $[Zn(L^1)]_4$ (**12**).

The environment about each zinc atom can be described as $[N_3S]$ distorted tetrahedral. Each zinc atom is coordinated to two anionic $[L^1]^{2-}$ ligands: one of them uses the amide and imine nitrogen atoms and the sulfur atom, while the other ligand uses the hydrazide nitrogen atom (Scheme 6).

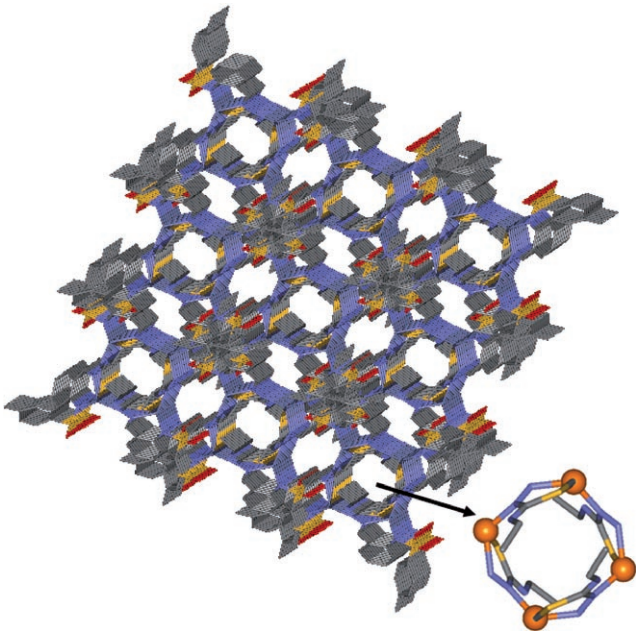

Figure 7. Porous structure shown by the crystal cell for the tetranuclear square complex $[Zn(L^1)]_4$ (**12**).

In addition, one of the O atoms of each tosyl group is close to one metal centre [Zn-O ≈2.459 Å]. The existence of these weak interactions, as well as the steric hindrance exerted by the terminal ethyl groups of a neighbouring ligand unit, clearly precludes the coordination of additional ligands.

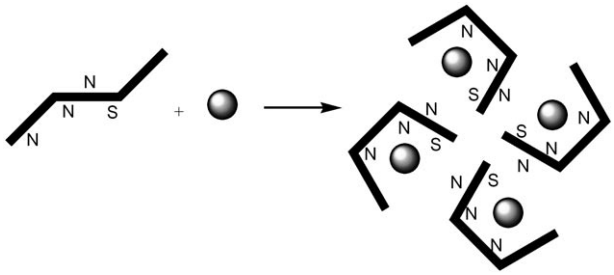

Scheme 6. Self-assembly of the tetranuclear complex $[Zn(L^1)]_4$ (**12**).

Conclusion

We have presented the formation of a new disulfide ligand by oxidation of a thiosemicarbazone. This reproducible process opens up a synthetic route that will allow the creation of a new library of disulfide ligands. Furthermore, the oxidation of thiosemicarbazones to disulfides may provide new information pertaining to the well-known biological properties of some thiosemicarbazone systems, above all those aspects related to their possible therapeutic uses.

Moreover, we have also presented a new thiosemicarbazone cyclisation process that is induced and catalysed by copper atoms. This catalytic process yields metal complexes derived from heterocyclic systems that could not be so easily obtained by conventional organic synthesis.

Thiosemicarbazone skeletons provide suitable coordinative environments for the generation of low-coordinated lead complexes in which the lone pair is stereochemically active.

The work presented herein also emphasises the versatility of thiosemicarbazones as building blocks allowing the assembly of interesting new supramolecular structures. In this context, it should be noted that Zn^{2+} ions induce a particular zeolite-type structure that may be capable of hosting small molecules or ions, presumably through hydrogen bonding.

Experimental Section

Materials: All solvents, 4-*N*-ethyl-3-thiosemicarbazide, and tetraethylammonium perchlorate are commercially available and were used without further purification. 2-Tosylaminobenzaldehyde was synthesised according to the published procedure.[12] Metals (Ega Chemie) were used as plates of approximate dimensions $2\times2\,cm^2$, except for manganese, which was employed in the form of platelets.

Physical measurements: Elemental analyses of C, H, N, and S were performed on a Fisons EA 1108 analyser. ^1H, ^{13}C, and multinuclear (^{113}Cd and ^{207}Pb) NMR spectra were recorded on Varian Mercury 300 and Bruker AMX-500 spectrometers respectively, using [D$_6$]DMSO as solvent. Chemical shifts are expressed relative to tetramethylsilane (^1H NMR), 0.1 M $Cd(ClO_4)_2$ (^{113}Cd NMR), and neat tetramethyllead using a saturated solution of $PbPh_4$ in $CDCl_3$ ($\delta=-178$ ppm) as an external reference (^{207}Pb NMR). Infrared spectra were measured from samples in KBr pellets on a Bruker IFS-66 V spectrophotometer in the range 4000–100 cm^{-1}. Fast atom bombardment mass spectra (FAB) were obtained on a Kratos MS-50 mass spectrometer, employing Xe atoms at 70 keV in *m*-nitrobenzyl alcohol as a matrix; electronic impact (EI) mass spectra were recorded on an HP 5988 A quadrupolar mass spectrometer and electrospray ionisation (ESI) mass spectra on an API 4000 Applied Biosystems mass spectrometer with triple quadrupole analyser. The conductivities of 10^{-3} M solutions in acetone were measured using a Crison micro CM 2200 conductivimeter. Room temperature magnetic measurements were performed using a Sherwood Scientific magnetic susceptibility balance, calibrated using mercury tetrakis(isothiocyanato)cobaltate(II). UV/Vis absorption spectra were recorded from solutions in acetonitrile in the concentration range 1×10^{-5}–5×10^{-5} M at room temperature using a Hewlett Packard 8452 A spectrophotometer. Steady-state corrected emission and excitation spectra were recorded with a Fluoromax-2 spectrofluorimeter using 4×10^{-7} M solutions in acetonitrile. Quantum yields were determined using quinine sulfate dihydrate in 1.0 N H_2SO_4 ($\Phi_F=0.546$) as a fluorescence standard.[49]

Ligand synthesis: *N*-{2-([4-*N*-Ethylthiosemicarbazone]methyl)phenyl}-*p*-toluenesulfonamide, H_2L^1, was prepared by condensation of 4-*N*-ethyl-3-thiosemicarbazide (0.43 g, 3.64 mmol) with 2-tosylaminobenzaldehyde (1.00 g, 3.64 mmol) in ethanol (150 mL). The solution was heated under reflux over a period of 5 h, concentrated to ≈30 mL in an apparatus fitted with a Dean–Stark trap, and then cooled over a period of 12 h (4 °C). The white solid formed was collected by filtration, washed with diethyl ether (2×5 mL), and dried in vacuo. Recrystallisation from a mixture of chloroform and acetone yielded colourless single crystals of **1**, which were suitable for X-ray diffraction analysis.

H_2L^1 (1): Yield 85 %; m.p. 206–208 °C; elemental analysis calcd (%) for $C_{17}H_{20}N_4O_2S_2$: C 54.2, H 5.3, N 14.9, S 17.0; found: C 54.1, H 5.5, N 15.1, S 16.9; EI-MS: *m*/*z* (%): 376 (100) [H_2L^1]; IR (KBr): $\tilde{\nu}$ = ν(NH) 3367 (w), 3151 (m), ν(C=N+C−N) 1602 (m), 1547 (s), $\nu_{asym}(SO_2)$ 1340 (s), $\nu_{sym}(SO_2)$ 1160 (s), ν(C=S) 1091 (m), 814 cm^{-1} (m); ^1H NMR ([D$_6$]DMSO): $\delta=11.47$ (s, 1H), 9.86 (s, 1H), 8.47 (t, 1H, $J=5.9$ Hz), 8.31 (s, 1H), 8.03 (dd, 1H, $J=5.6$, 3.9 Hz), 7.52 (d, 2H, $J=7.9$ Hz), 7.32 (d, 2H, $J=7.9$ Hz), 7.24 (d, 1H, $J=5.8$ Hz), 7.22 (d, 1H, $J=5.3$ Hz), 6.78 (dd, 1H, $J=5.3$, 3.8 Hz), 3.59 (q, 2H, $J=6.6$ Hz), 2.35 (s, 3H), 1.16 ppm (t, 3H, $J=6.6$ Hz); ^{13}C NMR ([D$_6$]DMSO): $\delta=176.64$ (C=S), 143.21 (C), 139.78 (HC=N), 136.41 (C), 134.92 (C), 130.81 (C), 129.81 (CH), 129.45 (2×CH), 127.32 (CH), 126.90 (2×CH), 126.61 (2×CH), 38.26 (CH_2), 20.95 (CH_3), 14.53 ppm (CH_3); UV/Vis (CH_3CN): λ_{max} (ε) = 222 (20340), 240 (sh, 14890), 320 nm (20840 $mol^{-1}\,dm^3\,cm^{-1}$).

Synthesis of the complexes: All complexes were synthesised by way of an electrochemical method,[8] which we have tailored to our needs.[50] The general procedure can be typified as follows: a solution of the ligand H_2L^1 in acetonitrile, containing about 10 mg of tetraethylammonium perchlorate as supporting electrolyte, is electrolysed using a platinum wire as the cathode and a metal plate as the anode. The cell can be summarised as: $Pt(-)\,|\,H_2L^1 + CH_3CN\,|\,M(+)$, where M = Mn, Fe, Co, Ni, Cu, Ag, Zn, Cd, Sn, and Pb. (**CAUTION**: Although no problems have been encountered in the course of our experiments, all perchlorate compounds are potentially explosive and should therefore be handled in small quantities and with great care!). The solids obtained were washed with diethyl ether and dried in vacuo.

It must be noted that during the electrochemical syntheses involving manganese and copper, different metal-catalysed processes took place with important consequences in relation to the ligand skeleton structure. In the electrochemical synthesis of the manganese complex, a new dithiolate ligand H_2L^2 was obtained as a side-product. In the case of copper, the main solid compound contained the initial ligand H_2L^1 and the product crystallised from the mother liquor showed the metal atoms coordinated to a new cyclised thiosemicarbazone ligand, H_2L^3. Unfortunately, the yield of the crystalline complex containing H_2L^3 was too low to be determined.

$[Mn(L^1)]_2$ (2): Yield 64 %; m.p. >300 °C; elemental analysis calcd (%) for $C_{34}H_{36}N_8O_4S_4Mn_2$: C 47.5, H 4.2, N 13.0, S 14.9; found: C 47.9, H 4.4, N 12.8, S 14.6; ESI-MS: *m*/*z*: 428.2 $[ML^1]^+$, 861.1 $[M_2L^1{}_2+H]^+$; IR (KBr): $\tilde{\nu}$ = ν(NH) 3367 (m), ν(C=N+C−N) 1609 (s), 1546 (s), $\nu_{asym}(SO_2)$ 1336 (m), $\nu_{sym}(SO_2)$ 1159 (s), ν(C−S) 1090 (s), 813 cm^{-1} (w); $\mu=6.0$ MB; $\Lambda_M=7.6\,\Omega^{-1}\,cm^2\,mol^{-1}$; UV/Vis ($CH_3CN$): λ_{max} (ε) = 224 (52583), 252 (sh, 28387), 302 (sh, 28920), 316 (32660), 332 (33793), 348 (sh, 26613 $mol^{-1}\,dm^3\,cm^{-1}$). Slow concentration of the mother liquor from the manganese electrochemical synthesis, followed by recrystallisation of the residue obtained from a dichloromethane/diethyl ether mixture, allowed the isolation of pale-yellow crystals of a new ligand, H_2L^2 (**3**), which was fully characterised, including the determination of its structure by X-ray diffraction analysis.

H_2L^2 (3): Yield 30 %; m.p. 183–185 °C; elemental analysis calcd (%) for $C_{34}H_{38}N_8O_4S_4$: C 54.3, H 5.1, N 14.9, S 17.1; found: C 54.2, H 5.4, N 15.0, S 17.0; ESI-MS: *m*/*z*: 752.2 $[H_2L^2+H]^+$, 376.1 $[H_2L^1]^+$; IR (KBr): $\tilde{\nu}$ = ν(NH) 3368 (s), 3357 (s), ν(C=N+C−N) 1609 (s), 1546 (s), $\nu_{asym}(SO_2)$ 1337 (s), $\nu_{sym}(SO_2)$ 1158 (s), ν(C−S) 1089 (m), 812 (w), ν(S−S) 481 cm^{-1} (m); ^1H NMR ([D$_6$]DMSO): $\delta=11.04$ (s, 2H), 8.45 (s, 2H), 7.72 (d, 4H, $J=7.3$ Hz), 7.59 (d, 2H, $J=8.0$ Hz), 7.41–7.24 (m, 8H), 7.12 (t, 2H, $J=7.3$ Hz), 6.96 (t, 2H, $J=5.8$ Hz), 3.48 (q, 4H, $J=6.6$ Hz), 2.32 (s, 6H), 1.15 ppm (t, 6H, $J=6.6$ Hz); UV/Vis (CH_3CN): λ_{max} (ε) = 224 (43640), 248 (sh, 23990), 302 (sh, 27230), 316 (33730), 334 (36750), 348 nm (sh, 30330 $mol^{-1}\,dm^3\,cm^{-1}$).

$[Fe(L^1)]_2\cdot4H_2O$ (4): Yield 65 %; m.p. >300 °C; elemental analysis calcd (%) for $C_{34}H_{44}N_8O_8S_4Fe_2$: C 43.8, H 4.7, N 12.0, S 13.8; found: C 43.6, H 4.6, N 11.8, S 13.2; ESI-MS: *m*/*z*: 431.0 $[ML^1+H]^+$, 861.1 $[M_2L^1{}_2]^+$; IR (KBr): $\tilde{\nu}$ = ν(OH+NH) 3397 (m), ν(C=N+C−N) 1597 (m), 1556 (m), $\nu_{asym}(SO_2)$ 1345 (w), $\nu_{sym}(SO_2)$ 1158 (m), ν(C−S) 1083 (m), 814 cm^{-1} (w); $\mu=5.3$ MB; $\Lambda_M=55.7\,\Omega^{-1}\,cm^2\,mol^{-1}$; UV/Vis ($CH_3CN$): λ_{max} (ε) = 226 (44704), 276 (24099), 303 (sh, 30013), 316 (31968), 332 nm (sh, 30268 $mol^{-1}\,dm^3\,cm^{-1}$).

$[Co(L^1)]_2\cdot0.5H_2O$ (5): Yield 52 %; m.p. >300 °C; elemental analysis calcd (%) for $C_{34}H_{37}N_8O_{4.5}S_4Co_2$: C 46.6, H 4.2, N 12.8, S 14.6; found: C 46.8,

H 4.2, N 12.8, S 14.7; ESI-MS: m/z: 434.0 $[ML^1+H]^+$, 866.0 $[M_2L^1{}_2]^+$; IR (KBr): $\tilde{\nu}$ = ν(OH) 3432 (w), ν(NH) 3348 (m), ν(C=N+C–N) 1598 (m), 1552 (m), $\nu_{asym}(SO_2)$ 1340 (m), $\nu_{sym}(SO_2)$ 1127 (s), ν(C–S) 1075 (s), 814 cm^{-1} (m); μ = 4.4 MB; Λ_M = 2.5 $\Omega^{-1}cm^2mol^{-1}$; UV/Vis (CH_3CN): λ_{max} (ε) = 228 (98609), 321 (sh, 40853), 340 (37969), 374 nm (29968 $mol^{-1}dm^3cm^{-1}$).

$[Ni(L^1)]_2$·0.5H_2O (6): Yield 63%; m.p. >300°C; elemental analysis calcd (%) for $C_{34}H_{37}N_8O_{4.5}S_4Ni_2$: C 46.6, H 4.2, N 12.8, S 14.7; found: C 46.9, H 4.2, N 12.9, S 14.1; ESI-MS: m/z: 433.0 $[ML^1]^+$, 861.1 $[M_2L^1{}_2+Na-2CH_3]^+$; IR (KBr): $\tilde{\nu}$ = ν(OH) 3416 (w), ν(NH) 3234 (w), ν(C=N+C–N) 1592 (m), 1561 (s), $\nu_{asym}(SO_2)$ 1342 (m), $\nu_{sym}(SO_2)$ 1134 (s), ν(C–S) 1082 (m), 815 cm^{-1} (w); μ = 3.2 MB; Λ_M = 2.7 $\Omega^{-1}cm^2mol^{-1}$; UV/Vis (CH_3CN): λ_{max} (ε) = 239 (105237), 286 (47571), 316 (45789), 376 nm (33036 $mol^{-1}dm^3cm^{-1}$).

$[Cu(L^1)]_2$·0.5H_2O (7): Yield 35%; m.p. >300°C; elemental analysis calcd (%) for $C_{34}H_{37}N_8O_{4.5}S_4Cu_2$: C 46.1, H 4.2, N 12.6, S 14.5; found: C 46.0, H 4.4, N 12.4, S 13.8; ESI-MS: m/z: 439.0 $[ML^1+H]^+$, 861.1 $[M_2L^1{}_2-CH_3]$ (100%); IR (KBr): $\tilde{\nu}$ = ν(OH) 3455 (w), ν(NH) 3395 (m), ν(C=N+C–N) 1596 (m), 1541 (s), $\nu_{asym}(SO_2)$ 1334 (m), $\nu_{sym}(SO_2)$ 1157 (s), ν(C–S) 1090 (m), 811 cm^{-1} (w); μ = 2.2 MB; Λ_M = 1.4 $\Omega^{-1}cm^2mol^{-1}$; UV/Vis (CH_3CN): λ_{max} (ε) = 222 (42453), 292 (21632), 334 (26067), 370 nm (19231 $mol^{-1}dm^3cm^{-1}$). Slow evaporation of the solvent from the mother liquor provided dark-green crystals of two new Cu^{II} complexes, $[Cu(L^3)]_2$·CH_3CN (**8**) and $[Cu(L^3)(H_2O)]_2$·CH_3CN·H_2O (**9**), which were also studied crystallographically.

$[Ag_2(L^1)]_2$·3H_2O (10): Yield 65%; m.p. >300°C; elemental analysis calcd (%) for $C_{34}H_{42}N_8O_7S_4Ag_4$: C 32.7, H 3.6, N 8.9, S 10.1; found: C 33.1, H 3.4, N 9.1, S 10.4; ESI-MS: m/z: 482.9 $[ML^1]^+$, 591.2 $[M_2L^1]^+$, 986.1 $[M_2L^1{}_2+Na]^+$, 1180.1 $[M_4L^1{}_2]^+$; IR (KBr): $\tilde{\nu}$ = ν(OH) 3470 (w), ν(NH) 3395 (w), ν(C=N+C–N) 1597 (m), 1529 (s), $\nu_{asym}(SO_2)$ 1333 (m), $\nu_{sym}(SO_2)$ 1157 (s), ν(C–S) 1089 (m), 812 cm^{-1} (w); ^{1}H NMR ([D$_6$]DMSO): δ = 7.68 (t, 1H, J = 7.6 Hz), 7.58–7.50 (m, 3H), 7.35 (t, 1H, J = 7.9 Hz), 7.26 (t, 1H, J = 4.8 Hz), 7.20–7.08 (m, 3H), 7.00 (d, 1H, J = 7.8 Hz), 3.57 (q, 2H, J = 7.0 Hz), 2.34 (s, 3H), 1.29 ppm (t, 3H, J = 7.0 Hz); Λ_M = 2.9 $\Omega^{-1}cm^2mol^{-1}$; UV/Vis (CH_3CN): λ_{max} (ε) = 226 (89670), 249 (sh, 57863), 298 (51838), 316 nm (54336 $mol^{-1}dm^3cm^{-1}$).

$[Zn(L^1)]_4$·2H_2O (11): Yield 50%; m.p. >300°C; elemental analysis calcd (%) for $C_{68}H_{76}N_{16}O_{10}S_8Zn_4$: C 45.5, H 4.2, N 12.5, S 14.3; found: C 45.1, H 4.4, N 12.0, S 13.7; ESI-MS: m/z: 439.0 $[ML^1]^+$, 879.9 $[M_2L^1{}_2]^+$, 1318.7 $[M_3L^1{}_3]^+$, 1757.9 $[M_4L^1{}_4]^+$; IR (KBr): $\tilde{\nu}$ = ν(OH) 3419 (w), ν(NH) 3362 (w), ν(C=N+C–N) 1599 (m), 1556 (m), $\nu_{asym}(SO_2)$ 1340 (m), $\nu_{sym}(SO_2)$ 1127 (s), ν(C–S) 1079 (s), 813 cm^{-1} (w); ^{1}H NMR ([D$_6$]DMSO): δ = 8.25 (s, 1H), 7.70 (d, 2H, J = 7.9 Hz), 7.33 (d, 1H, J = 6.9 Hz), 7.31–7.22 (m, 3H), 7.16 (t, 1H, J = 4.8 Hz), 7.09 (t, 1H, J = 7.4 Hz), 6.85 (t, 1H, J = 7.4 Hz), 3.19 (q, 2H, J = 7.3 Hz), 2.30 (s, 3H), 1.12 ppm (t, 3H, J = 7.3 Hz); Λ_M = 4.0 $\Omega^{-1}cm^2mol^{-1}$; UV/Vis (CH_3CN): λ_{max} (ε) = 224 (86540), 266 (sh, 41490), 314 (sh, 35510), 330 (44340), 358 (49270), 374 nm (sh, 41550 $mol^{-1}dm^3cm^{-1}$). Recrystallisation of $[Zn(L^1)]_4$·2H_2O from the mother liquor yielded colourless crystals of **12**, which were studied by X-ray diffraction analysis.

$[Cd(L^1)]_2$·CH_3CN (13): Yield 62%; m.p. >300°C; elemental analysis calcd (%) for $C_{36}H_{39}N_9O_4S_4Cd_2$: C 42.6, H 3.8, N 12.4, S 12.6; found: C 42.2, H 4.1, N 12.2, S 12.3; ESI-MS: m/z: 487.0 $[ML^1]^+$, 864.0 $[ML^1{}_2]^+$, 972.9 $[M_2L^1{}_2]^+$; IR (KBr): $\tilde{\nu}$ = ν(NH) 3373 (w), ν(C=N+C–N) 1598 (m), 1516 (s), $\nu_{asym}(SO_2)$ 1336 (m), $\nu_{sym}(SO_2)$ 1125 (s), ν(C–S) 1080 (s), 813 cm^{-1} (w); ^{1}H NMR ([D$_6$]DMSO): δ = 8.15 (s, 1H), 7.63 (d, 2H, J = 7.5 Hz), 7.25–7.15 (m, 4H), 7.01 (t, 1H, J = 7.7 Hz), 6.83 (t, 1H, J = 7.7 Hz), 6.69 (t, 1H, J = 4.8 Hz), 3.18 (q, 2H, J = 7.3 Hz), 2.28 (s, 3H), 1.15 ppm (t, 3H, J = 7.3 Hz); ^{113}Cd NMR ([D$_6$]DMSO): δ = 257.9 ppm; Λ_M = 13.6 $\Omega^{-1}cm^2mol^{-1}$; UV/Vis (CH_3CN): λ_{max} (ε) = 222 (40275), 266 (19513), 314 (sh, 15183), 328 (sh, 17421), 356 (20863), 374 nm (17079 $mol^{-1}dm^3cm^{-1}$).

$[Pb(L^1)]_2$·3H_2O (14): Yield 67%; m.p. >300°C; elemental analysis calcd (%) for $C_{34}H_{42}N_8O_7S_4Pb_2$: C 33.5, H 3.4, N 9.2, S 10.5; found: C 33.2, H 3.2, N 9.1, S 10.1; ESI-MS: m/z: 583.1 $[ML^1+2H]^+$, 959.2 $[ML^1{}_2]^+$, 1163.1 $[M_2L^1{}_2]^+$; IR (KBr): $\tilde{\nu}$ = ν(OH) 3405 (w), ν(NH) 3271 (m), ν(C=N+C–N) 1595 (m), 1521 (s), $\nu_{asym}(SO_2)$ 1342 (m), $\nu_{sym}(SO_2)$ 1122 (s), ν(C–S) 1074 (s), 810 cm^{-1} (m); ^{1}H NMR ([D$_6$]DMSO): δ = 8.01 (s, 1H), 7.81 (d, 2H, J = 7.9 Hz), 7.33 (d, 1H, J = 8.5 Hz), 7.29–7.19 (m, 3H), 7.09 (t, 1H, J = 7.4 Hz), 6.72 (t, 1H, J = 7.4 Hz), 6.67 (t, 1H, J = 4.7 Hz), 3.27 (q, 2H, J = 7.1 Hz), 2.29 (s, 3H), 1.11 ppm (t, 3H, J = 7.1 Hz); ^{207}Pb NMR ([D$_6$]DMSO): δ = –236.9 ppm; Λ_M = 4.7 $\Omega^{-1}cm^2mol^{-1}$; UV/Vis (CH_3CN): λ_{max} (ε) = 226 (72620), 270 (37830), 328 (23605), 396 nm (9120 $mol^{-1}dm^3cm^{-1}$). Slow concentration of the mother liquor yielded orange crystals of $[Pb(L^1)]_2$ (**15**), which were characterised by X-ray diffraction analysis.

X-ray crystallographic studies: Crystals of **1**, **3**, **8**, **9**, **12**, and **15** were grown as described above. The main crystallographic data for these compounds are summarised in Table 2 and Table 3. Data for **1** were collected on an FRS91-Kappa CCD 2000 Bruker Nonius diffractometer using graded mirror-monochromated $Cu_{K\alpha}$ radiation (λ = 1.5418 Å) from a ro-

Table 2. Crystal data and structure refinement for H_2L^1 (**1**) and H_2L^2 (**3**).

	H_2L^1 (**1**)	H_2L^2 (**3**)
empirical formula	$C_{17}H_{20}N_4O_2S_2$	$C_{34}H_{38}N_8O_4S_4$
crystal size [mm]	0.95×0.53×0.48	0.44×0.09×0.08
formula weight	376.49	750.96
crystal system	monoclinic	monoclinic
space group	$P2(1)/c$	$P2(1)/c$
a [Å]	13.150(1)	17.865(3)
b [Å]	5.6677(9)	13.554(2)
c [Å]	24.781(4)	16.122(3)
α [°]	90	90
β [°]	90.786(8)	112.967(2)
γ [°]	90	90
V [Å^3]	1846.8(5)	3594.4(1)
T [K]	293(2)	110(2)
Z	4	4
μ [mm^{-1}]	2.768	0.315
reflections collected	29669	30202
independent reflections [R_{int}]	3590 [0.1003]	7058 [0.0526]
$R1$, $wR2$ [$I>2\sigma(I)$]	0.0567, 0.1346	0.0400, 0.0949
$R1$, $wR2$ (all data)	0.0583, 0.1371	0.0675, 0.1043

Table 3. Crystal data and structure refinement for **8**, **9**, and **15**.

	$[Cu(L^3)]_2$·CH_3CN (**8**)	$[Cu(L^3)(H_2O)]_2$ ·CH_3CN·H_2O (**9**)	$[Pb(L^1)]_2$ (**15**)
empirical formula	$C_{40}H_{41}N_{11}O_6S_4Cu_2$	$C_{40}H_{45}N_{11}O_8S_4Cu_2$	$C_{34}H_{36}N_8O_4S_4Pb_2$
crystal size [mm]	0.24×0.13×0.09	0.46×0.2×0.1	0.49×0.3×0.19
formula weight	1027.08	1081.23	1163.37
crystal system	triclinic	triclinic	monoclinic
space group	$P\bar{1}$	$P\bar{1}$	$P\bar{1}$
a [Å]	8.844(15)	8.841(5)	8.708(2)
b [Å]	9.933(16)	10.985(5)	10.569(2)
c [Å]	14.13(2)	13.333(5)	10.963(2)
α [°]	70.37(3)	104.400(5)	78.131(4)
β [°]	86.89(3)	99.499(5)	79.032(4)
γ [°]	73.14(3)	93.359(5)	85.183(4)
V [Å^3]	1118(3)	1230.3(10)	968.3(4)
T [K]	293(2)	293(2)	293(2)
Z	2	2	2
μ [mm^{-1}]	1.202	1.103	8.946
reflections collected	13121	14072	11971
independent reflections [R_{int}]	4706 [0.0421]	5003 [0.0232]	3671 [0.0237]
$R1$, $wR2$ [$I>2\sigma(I)$]	0.0400 [0.0953]	0.0267 [0.0659]	0.0170 [0.0428]
$R1$, $wR2$ (all data)	0.0727 [0.1128]	0.0318 [0.0688]	0.0191 [0.0435]

tating anode generator. The cell refinement was carried out by means of HKL Denzo and Scalepack[51] and the data reduction by SAINT.[52] Data for **3**, **8**, **9**, and **12** were collected on a Smart CCD-1000 Bruker diffractometer, using graphite-monochromated $Mo_{K\alpha}$ radiation ($\lambda = 0.71073$ Å) from a fine-focus sealed-tube source. Computing and data reduction were carried out using SAINT software in all of these cases.[52] The structures of **1**, **3**, **8**, and **12** were solved by SIR97 or SIR92,[53] while DIRDIF-99[54] was used for **9**. The structures of all these complexes were finally refined by full-matrix, least-squares techniques based on F^2 using SHELXL.[55] In all cases, an empirical absorption correction was applied using SADABS.[56] All non-hydrogen atoms were anisotropically refined except for the disordered atoms in **1**. Some hydrogen atoms were included in the model at geometrically calculated positions and refined using a riding model, and some were refined by electronic density. Data for **15** were collected on a Bruker X8 Kappa CCD-APEX III diffractometer using graphite-monochromated $Mo_{K\alpha}$ radiation ($\lambda = 0.71073$ Å) from a fine-focus sealed-tube source. Computing and data reduction were performed using the SAINT software[52] and the preliminary structure solution was performed with SIR92.[53] Structural data are not included in this manuscript but we are completely sure of the gross structural features shown in this work.

CCDC-649340–649344 contain the supplementary crystallographic data for this paper. These data can be obtained free of charge from The Cambridge Crystallographic Data Centre via www.ccdc.cam.ac.uk/data_request/cif.

Acknowledgements

The authors would like to thank the Xunta de Galicia (PGIDIT06PXIB20901PR) and the Ministerio de Educación y Ciencia (CTQ2007–62485/BQU) for financial support. R.P. thanks the Xunta de Galicia for an Isidro Parga Pondal contract. M.J.R. thanks the Universidade de Santiago de Compostela for a predoctoral fellowship.

[1] J. S. Casas, M. S. García-Tasende, J. Sordo, *Coord. Chem. Rev.* **2000**, *209*, 197–261.
[2] D. X. West, A. E. Liberta, S. B. Padhye, R. C. Chitake, P. B. Sonawane, A. S. Kumbhar, R. G. Yerande, *Coord. Chem. Rev.* **1993**, *123*, 49–71.
[3] M. Vázquez, L. Fabbrizzi, A. Taglietti, R. M. Pedrido, A. M. González-Noya, M. R. Bermejo, *Angew. Chem.* **2004**, *116*, 1996; *Angew. Chem. Int. Ed.* **2004**, *43*, 1962–1965.
[4] S. N. Pandeya, D. Siram, G. Nath, E. DeClercq, *Eur. J. Pharm. Sci.* **1999**, *9*, 25–31, and references therein.
[5] A. C. Quiroga, C. Navarro-Ranninger, *Coord. Chem. Rev.* **2004**, *248*, 119–133.
[6] J. Easmon, G. Purstinger, G. Heinisch, T. Roth, H. H. Fiebig, W. Holzer, W. Jager, M. Jenny, J. Hoffmann, *J. Med. Chem.* **2001**, *44*, 2164–2171.
[7] G. Nocentini, *Crit. Rev. Oncol. Hematol.* **1996**, *22*, 89–126.
[8] C. Oldham, D. G. Tuck, *J. Chem. Educ.* **1982**, *59*, 420–421.
[9] a) M. Vázquez, M. R. Bermejo, M. Fondo, A. M. González, J. Mahía, L. Sorace, D. Gatteschi, *Eur. J. Inorg. Chem.* **2001**, 1863–1868; b) M. Vázquez, M. R. Bermejo, M. Fondo, A. García-Deibe, A. M. González, R. Pedrido, *Eur. J. Inorg. Chem.* **2002**, 465–472; c) M. Vázquez, M. R. Bermejo, J. Sanmartín, A. M. García-Deibe, C. Lodeiro, J. Mahía, *J. Chem. Soc. Dalton Trans.* **2002**, 870–877; d) M. Vázquez, M. R. Bermejo, M. Fondo, A. M. García-Deibe, A. M. González, R. Pedrido, J. Sanmartín, *Z. Anorg. Allg. Chem.* **2002**, 628, 1068–1074; e) M. R. Bermejo, M. Vázquez, J. Sanmartín, A. M. García-Deibe, M. Fondo, C. Lodeiro, *New J. Chem.* **2002**, *26*, 1365–1370; f) M. Vázquez, A. Taglietti, D. Gatteschi, L. Sorace, C. Sangregorio, A. M. González, M. Maneiro, R. Pedrido, M. R. Bermejo, *Chem. Commun.* **2002**, 1840–1841; g) M. Vázquez, M. R. Bermejo, M. Fondo, A. M. García-Deibe, J. Sanmartín, R. Pedrido, L. Sorace, D. Gatteschi, *Eur. J. Inorg. Chem.* **2003**, 1128–1135; h) R. Pedrido, M. R. Bermejo, A. M. García-Deibe, A. M. González-Noya, M. Maneiro, M. Vázquez, *Eur. J. Inorg. Chem.* **2003**, 3193–3200.
[10] M. R. Bermejo, A. M. González-Noya, R. M. Pedrido, M. J. Romero, M. Vázquez, *Angew. Chem.* **2005**, *117*, 4254–4259; *Angew. Chem. Int. Ed.* **2005**, *43*, 1962–1965.
[11] a) R. Pedrido, M. R. Bermejo, M. J. Romero, M. Vázquez, A. M. González-Noya, M. Maneiro, M. J. Rodríguez, M. I. Fernández, *Dalton Trans.* **2005**, 572–579; b) M. R. Bermejo, A. M. González-Noya, M. Martínez-Calvo, R. Pedrido, M. J. Romero, M. I. Fernández, M. Maneiro, *Z. Anorg. Allg. Chem.* **2007**, *633*, 807–813.
[12] a) N. I. Chernova, Y. S. Ryabokobylko, V. G. Brudz, B. M. Bolotin, *Zh. Org. Khim.* **1971**, *7*, 1680–1687; b) J. Mahía, M. Maestro, M. Vázquez, M. R. Bermejo, A. M. González, M. Maneiro, *Acta Crystallogr. Sect. A* **1999**, *C55*, 2158–2160.
[13] M. Morioka, M. Kato, H. Yoshida, T. Ogata, *Heterocycles* **1997**, *45*, 1173–1181.
[14] K. Nakamoto, *Infrared and Raman Spectra of Inorganic and Coordination Compounds*, Wiley, New York, **1997**.
[15] N. G. Charles, E. A. H. Griffith, P. F. Rodesiler, E. L. Amma, *Inorg. Chem.* **1983**, *22*, 2717–2723, and references therein.
[16] a) B. Wrackmeyer, K. Horchler, *Annu. Rep. NMR Spectrosc.* **1989**, *22*, 249–304; b) J. M. Aramini, T. Hiraoki, M. Yazawa, T. Yuan, M. Zhang, H. J. Vogel, *J. Biol. Inorg. Chem.* **1996**, *1*, 39–48.
[17] G. D. Fallon, L. Spiccia, B. O. West, Q. Zhang, *Polyhedron* **1997**, *16*, 19–23.
[18] J. Sanchiz, P. Esparza, D. Villagra, S. Domínguez, A. Mederos, F. Brito, L. Araujo, A. Sánchez, J. M. Arrieta, *Inorg. Chem.* **2002**, *41*, 6048–6055.
[19] L. Prodi, F. Bolletta, M. Montalti, N. Zaccheroni, *Coord. Chem. Rev.* **2000**, *205*, 59–83.
[20] F. Wu, S. W. Bae, J. Hong, *Tetrahedron Lett.* **2006**, *47*, 8851–8854.
[21] a) S. Aoki, K. Sakurama, N. Matsuo, Y. Yamada, R. Takasawa, S. Tanuma, M. Shiro, K. Takeda, E. Kimura, *Chem. Eur. J.* **2006**, *12*, 9066–9080; b) R. Métivier, I. Leray, B. Valeur, *Chem. Eur. J.* **2004**, *10*, 4480–4490.
[22] a) S. Furberg, J. Solbakk, *Acta Chem. Scand.* **1973**, *27*, 236–238; b) N. V. Raghavan, K. Seff, *Acta Cryst.* **1977**, *B33*, 386–391.
[23] E. Shefter, *J. Chem. Soc. B* **1970**, 903–906.
[24] L. S. Higashi, M. Lundeen, K. Seff, *J. Am. Chem. Soc.* **1978**, *100*, 8101–8106.
[25] J. A. McCleverty, T. J. Meyer, Comprehensive Coordination Chemistry II, Elsevier, Amsterdam, The Netherlands, **2004**.
[26] a) S. Patay, The Chemistry of the Thiol Group, Wiley, London, **1984**, Parts 1 and 2; b) E. I. Stiefel, K. Matsumoto, *Transition Metal Sulfur Chemistry*, American Chemical Society, Washington DC, **1996**.
[27] a) P. E. G. Ferrer, A. M. Williams, E. C. Castellano, O. E. Z. Piro, *Z. Anorg. Allg. Chem.* **2002**, *628*, 1979–1984; b) S. Itoh, M. Nagagawa, S. Fukuzumi, *J. Am. Chem. Soc.* **2001**, *123*, 4087–4088.
[28] T. Osako, Y. Ueno, Y. Tachi, S. Itoh, *Inorg. Chem.* **2004**, *43*, 6516–6518.
[29] P. J. Blower, J. R. Dilworth, *Coord. Chem. Rev.* **1987**, *76*, 121–185.
[30] a) E. López-Torres, M. A. Mendiola, *Polyhedron* **2005**, *24*, 1435–1444; b) E. López-Torres, M. A. Mendiola, C. J. Pastor, *Inorg. Chem.* **2006**, *45*, 3103–3112.
[31] a) J. Tallón, J. A. García-Vázquez, J. Romero, M. S. Louro, A. Sousa, Q. Chen, Y. Chang, J. Zubieta, *Polyhedron* **1995**, *14*, 2309–2317; b) J. A. Castro, J. Romero, J. A. García-Vázquez, A. Castiñeiras, A. Sousa, J. Zubieta, *Polyhedron* **1995**, *14*, 2841–2847.
[32] A. Castiñeiras, I. García-Santos, S. Dehnen, P. Sevillano, *Polyhedron* **2006**, *25*, 3653–3660.
[33] M. Ravindranathan, N. Kalyanam, S. Sivaram, *J. Org. Chem.* **1982**, *47*, 4812–4813.
[34] R. Luo, X. Mao, Z. Pan, Q. Luo, *Spectrochim. Acta* **2000**, *56*, 1675–1680, and references therein.
[35] S. V. Ley, A. W. Thomas, *Angew. Chem.* **2003**, *115*, 5558–5607; *Angew. Chem. Int. Ed.* **2003**, *42*, 5400–5449.
[36] A. W. Addison, T. N. Rao, J. Reedijk, J. Van Rijn, G. C. Verschoor, *J. Chem. Soc. Dalton Trans.* **1984**, 1349–1356.

[37] M. Dobosz, A. Pachuta-Stec, *Acta Pol. Pharm.* **1996**, *53*, 123–131.
[38] L. Korzycka, M. Glowka, J. Janicka, *Pol. J. Chem.* **1998**, *72*, 73–77.
[39] R. Noto, P. L. Meo, M. Gruttadauria, G. J. Weber, *J. Heterocycl. Chem.* **1999**, *36*, 667–674, and references therein.
[40] M. Gruttadauria, F. Buccheri, P. L. Meo, R. Noto, G. J. Weber, *J. Heterocycl. Chem.* **1993**, *30*, 765–770.
[41] J. S. Casas, M. V. Castaño, M. S. García-Tasende, E. Rodríguez-Castellón, A. Sánchez, L. M. Sanjuán, J. Sordo, *Dalton Trans.* **2004**, 2019–2026, and references therein.
[42] a) L. Somogyi, *Liebigs Ann. Chem.* **1991**, 1267–1271; b) R. Milcent, T.-H. Nguyen, *J. Heterocycl. Chem.* **1986**, *23*, 881–883; c) J. S. Casas, M. V. Castaño, E. E. Castellano, J. Ellena, M. S. García-Tasende, A. Gato, A. Sánchez, L. M. Sanjuán, J. Sordo, *Inorg. Chem.* **2002**, *41*, 1550–1557.
[43] a) P. Gómez-Saiz, J. García-Tojal, M. A. Maestro, F. J. Arnáiz, T. Rojo, *Inorg. Chem.* **2002**, *41*, 1345–1347; b) P. Gómez-Saiz, J. García-Tojal, V. Díez-Gómez, R. Gil-García, J. L. Pizarro, M. I. Arriortúa, T. Rojo, *Inorg. Chem. Commun.* **2005**, *8*, 258–262.
[44] P. Gómez-Saiz, R. Gil-García, A. Maestro, J. L. Pizarro, M. I. Arriortúa, L. Lezama, T. Rojo, J. García-Tojal, *Eur. J. Inorg. Chem.* **2005**, 3409–3413.
[45] N. V. Sidgwick, H. M. Powell, *Proc. R. Soc. London Ser. A* **1940**, *176*, 153–180.
[46] R. D. Hancock, M. S. Shaikfee, S. M. Dobson, J. C. A. Boeyens, *Inorg. Chim. Acta* **1988**, *154*, 229–238.
[47] R. Pedrido, M. J. Romero, M. R. Bermejo, A. M. González-Noya, M. Maneiro, M. J. Rodríguez, G. Zaragoza, *Dalton Trans.* **2006**, 5304–5314.
[48] G. B. Gardner, D. Venkataraman, J. S. Moore, S. Lee, *Nature* **1995**, *374*, 792–795.
[49] a) W. H. Melhuish, *J. Phys. Chem.* **1961**, *65*, 229–235; b) J. N. Demas, G. A. Crosby, *J. Phys. Chem.* **1971**, *75*, 991–1024.
[50] M. R. Bermejo, A. M. González, M. Fondo, A. García-Deibe, M. Maneiro, J. Sanmartín, O. L. Hoyos, M. Watkinson, *New J. Chem.* **2000**, *24*, 235–241.
[51] Z. Otwinowski, W. Minor, *Macromolecular Crystallography Pt. A* **1997**, *276*, 307–326.
[52] SAINT, *Siemens area detector integration software*, Bruker AXS Inc., Madison, WI, USA, **2003**.
[53] a) A. Altornare, G. Gascarano, C. Giacovazzo, A. Guagliardi, *J. Appl. Crystallogr.* **1993**, *26*, 343–350; b) A. Altornare, M. C. Burla, M. Carnalli, G. Cascarano, C. Giacovazzo, A. Guagliardi, A. G. G. Moliterni, G. Polidori, R. Spagan, *J. Appl. Crystallogr.* **1999**, *32*, 115–122.
[54] P. T. Beurskens, G. Admiraal, G. Beurskens, W. P. Bosman, R. de Gelder, R. Israel, J. M. M. Smith, DIRDIF99, University of Nijmegen, The Netherlands, **1999**.
[55] G. M. Sheldrick, SHELX-97 (SHELXS-97 and SHELXL-97), *Programs for Crystal Structure Analyses*, University of Göttingen, Germany, **1998**.
[56] G. M. Sheldrick, *SADABS*, *Program for Scaling and Correction of Area Detector Data*, University of Göttingen, Germany, **1996**.

Received: June 6, 2007
Published online: October 8, 2007

